

A GENERAL MULTI-PLANE MODEL FOR POST-LIQUEFACTION OF SAND*

S. A. SADRNEJAD

Dept. of Civil Engineering, K.N.Toosi University of Technology, Teheran, I. R. of Iran
Email: sadrnejad@hotmail.com

Abstract– A multi-plane model for the post-liquefaction of the undrained behaviour of sand is presented. The model incorporates the critical/steady state concept that postulates the existence of a state where sand continuously deforms at a certain constant effective stress depending two main parameters of both initial bulk parameters (i.e. void ratio or relative density) and stress level (i.e. mean stress). The local instability of saturated sand within post-liquefaction is highly dependent on the residual inherent/induced anisotropy, bedding plane effects, and stress/strain path.

Most of the models developed using stress/strain invariants are not capable of identifying the parameters depending on orientation such as fabric. This is mainly because stress/strain invariants are quantities similar to scalar quantities and not capable of carrying directional information with themselves.

The constitutive equations of the model are derived within the context of the non-linear elastic behaviour of the whole medium and the plastic sliding of interfaces of predefined multi-planes.

The proposed multi-plane based model is capable of predicting the behaviour of soils on the basis of plastic sliding mechanisms, elastic behaviour of particles and possibilities to see the micro-fabric effects as natural anisotropy as well as induced anisotropy in plasticity. The model is capable of predicting the behaviour of soil under different orientations of the bedding plane, and the history of strain progression during the application of any stress/strain paths. The influences of the rotation of the direction of principal stress and strain axes and induced anisotropy are included in a rational way without any additional hypotheses. The spatial strength distribution at a location as an approximation of the probable mobilized sliding mechanism is presented by an ellipsoid function built up on the bedding plane.

Keywords– Post-liquefaction, multi-plane, elastic-plastic, local instability

1. INTRODUCTION

Li and Dafalias [1] pointed out that the classical stress dilatancy approach in its exact form ignored the extra energy loss due to the static and dynamic constraints at particle contacts and led to a unique relationship between the stress ratio and dilatancy. Furthermore, it has been shown by Manzari and Dafalias [2], Wan *et al.* [3], and Li and Dafalias [4] that in order to model sand behaviour over a full range of density states, the additional dependence of dilatancy on the material internal states, and the sliding mechanism are needed. Further, the material state must be described in reference to the critical/steady state line [5, 6]. Accordingly, any local sliding instability may take its limited share in global behaviour and through a properly controlled scheme, the possibility of the deformability of a post-liquefied zone will proceed.

In addition, due mainly to the process of deposition under earth gravity, the behaviour of insitu sand is inherently anisotropy, meaning the stress-strain-strength relations for the same sand may vary as the stress tensor rotates relative to the orientation of the soil fabric. The observation and experiment on the flow-type behaviour of liquefied soil has revealed that the influence of inherent fabric anisotropy on the residual

*Received by the editors April 12, 2004; final revised form January 22, 2006.

strength of a granular soil is so drastic that the inherent anisotropy can no longer be ignored in sand modeling. The influence of fabric anisotropy has been known since the emergence of the geo-mechanics [7]. However, anisotropy manifested itself through the directional dependence of deformation characteristics of granular materials which has been widely documented in the literature [8, 9]. Furthermore, the degree of anisotropy may vary quite significantly, depending on the soil composition, or even other sources such as electro-chemical properties of pore water, consolidation history, etc. Given the intrinsic oriented nature of the soil fabric, it is important to include the effect of anisotropy in a rational way. The major obstacles, in this respect, are our ability to properly define the spatial and temporal variations of the soil properties, deformabilities, hardening and boundary conditions. The value of a model lies primarily in its ability to capture the basic trends in the material behaviour and thereby provide a more realistic representation of the problem.

However, more than just the fabric property of natural soil, the response of granular materials to a given stress depends on the orientation of that stress, whether, the particles alignment is constituted in a river, beach, coastal sands or artificially deposited sands. This phenomenon was also observed in a random arrangement of constituent glass balls, in which there is no obvious effects of fabric on the composition by Oda, [10-15]. This feature is, in general, known to be due to gravity and the motion tendency of the constituent particles towards the earth centre. This tendency can actually affect the geometry of the contact points of each particle no matter the shape and particle sizes. Induced anisotropy is generally initiated and constructed during plastic shear deformation and plays a key role in understanding the plastic behaviour of granular soil in a general stress state, including the rotation of principal stress axes (e.g. Sadrnejad, [16-20]).

In this study, a certain function of local strength variation is defined that depends on the overall causes of inherent anisotropy at that location. This function can present the maximum shear to normal stress as $\tan(\phi)$ in any probable sliding direction through the medium. Consequently, any change in the major principal stress axis direction is faced on new sets of maximum strengths against the sliding mechanism of grains.

2. STRAIN DISTRIBUTION AROUND A POINT

In general continuum mechanics, to define strain distribution at a point, the components are simply considered on the outer surface of a typical dx , dy , dz element. This method makes the solution to be considered uniform and the homogeneous strain distribution of the nine components over the outer surface of such dx , dy , dz element on three perpendicular coordinate axes. There is a further consideration in addition to the requirement that the displacements of a granular medium provide due to slippage/widening/closing between particles that make a contribution to the strain in addition to that from the compression of particles. Consider two neighbouring points on either side of the point of contact of two particles. These two points do not in general remain close to each other but describe complex trajectories. Fictitious average points belonging to the fictitious continuous medium can be defined which remain adjacent so as to define a strain tensor. The problem presents itself differently for disordered particles compared with the ordered sphere of equal sizes. In this case, small zones may even appear in which there is no relative movement of particles. This can lead to specific behaviour such as periodic instabilities known as slip-stick, creating non-homogeneity in strains and displacements.

The effects of non-homogeneity in the mechanical behaviour of non-linear materials are very important and must somehow be considered. Furthermore, these non-homogeneities are mostly neglected in mechanical testing because strains and stresses are usually measured at the boundary of the samples and therefore have to be considered reasonably within the whole volume.

Solving non-linear problems, the mechanical behaviour depends strongly on the stress/strain path as well as their histories. Upon these conditions, it may be claimed that the consideration of strain components along three perpendicular coordinate axes may not reflect the real historical changes during the loading procedure. In the most extreme case, the definition of a sphere shape element dr (instead of dx , dy , dz cube) carrying distributed strain similarly on its surface can reflect strain components on infinite orientation at a point when dr tends to zero.

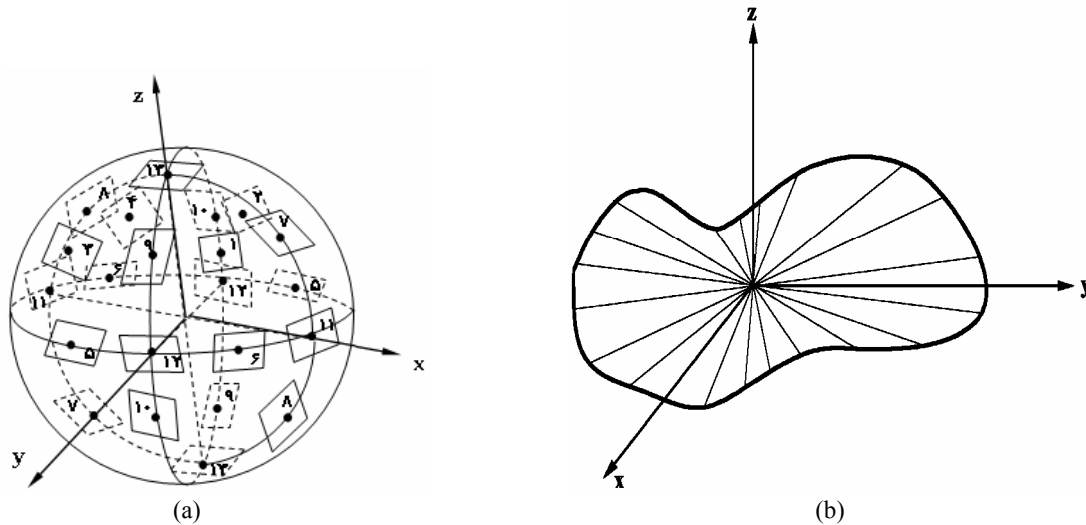


Fig. 1. a) Sphere elements, b) Typical deformed element

The finite strain at any point in three dimensions by coordinates (x, y, z) relate to the displacements of the sides of an initial rectangular-coordinate box with sides of length dx , dy , and dz to form the three sides of a parallelepiped. This configuration of strain is established by considering the displacements of the corner points $(x, 0, 0)$, $(0, y, 0)$, and $(0, 0, z)$. This kind of strain approach leads to defining a (3×3) strain tensor including six components to present the displacement gradient matrix at a node. Accordingly, any displacement and corresponding gradient have to be defined as independent components on three perpendicular coordinate axes.

Figure 1 shows sphere elements and a typical deformed shape. Obviously there is a certain history of displacement on any random orientation through the element. These are abbreviated in three, when a box - shape element is employed. To avoid not missing any directional information of strain, a spherical element carrying strain components over its surface as tangent and normal to the surface must be employed. This form of strain, which certainly represents a better distribution includes all directional information. Certainly, to obtain the strain components as presented on planes around box element, strain variation is integrated over the sphere surface. However, a predefined numerical integration may be employed to ease the solution. Numerical integration generally simulates the smooth curved sphere surface to a composition of flat tangential planes, making an approximated polygon to sphere surface. The higher the number of sampling planes, the closer is the approximated surface to the sphere. Clearly, if the number of sampling planes is taken as six, the approximated surface is the same as the normal dx , dy , dz box element.

3. MULTI-PLANE FRAMEWORK

Grains in a granular materials consisting of contacts and surrounding voids are particulate media that are mostly considered continuum for ease. The accurate behaviour of such particulate materials is to be investigated through micro-mechanics. However, the micro-mechanical behaviour of granular materials is

therefore inherently discontinuous and heterogeneous. The macroscopic as an overall or averaged behaviour of granular materials is determined not only by how discrete grains are arranged through the medium, but also by what kinds of interactions are operating among them. To investigate the micro-mechanical behaviour of granular materials, certainly the spatial distribution of contact points and orientation of grains must be identified. From an engineering point of view, the main goal is to formulate the macro-behaviour of granular materials in terms of micro-quantities. However, two well-known theories exist which explain the relation between micro-fields and macro-fields as macro-micro relations in a consistent manner as the average field theory and the homogenization theory.

For a granular material such as sand that supports the overall applied loads through contact friction, the overall mechanical response ideally may be described on the basis of the micro-mechanical behaviour of grains interconnections. Naturally this requires the description of overall stress, the characterization of fabric, representation of kinematics, development of local rate constitutive relations and evaluation of the overall differential constitutive relations in terms of the local quantities. The representation of the overall stress tensor in terms of micro level stresses and the condition, number and magnitude of contact forces has long been the aim of numerous researchers [21, 22].

Multi-plane framework, by defining the small continuum structural units as an assemblage of particles and voids that fill infinite spaces between the sampling planes, has appropriately justified the contribution of interconnection forces in overall macro-mechanics. Upon these assumptions, plastic deformations are likely to occur due to sliding, separation/closing of the boundaries and elastic deformations which are the overall responses of structural unit bodies. Therefore, the overall deformation of any small part of the medium is composed of the total elastic response and an appropriate summation of sliding, and the separation/closing phenomenon under the current effective normal and shear stresses on sampling planes. These assumptions adopt overall sliding, separation/closing of inter-granular points of grains included in one structural unit are summed up and contributed as a result of sliding and separation/closing surrounding boundary planes. This simply implies yielding/failure or even ill-conditioning and bifurcation response is possible over any of the randomly oriented sampling planes. Consequently, plasticity control such as yielding should be checked at each of the planes and those of the planes that are sliding will contribute to plastic deformation. Therefore, the granular material mass has an infinite number of yield functions usually one for each of the planes in the physical space.

Figure 2 shows the arrangement of artificial polyhedron simulated by real soil grains. The created polyhedrons have roughly 13 sliding planes, passing through each point in the medium. The location of tip heads of normal to the planes defining corresponding direction cosines are shown on the surface of the unit radius sphere.

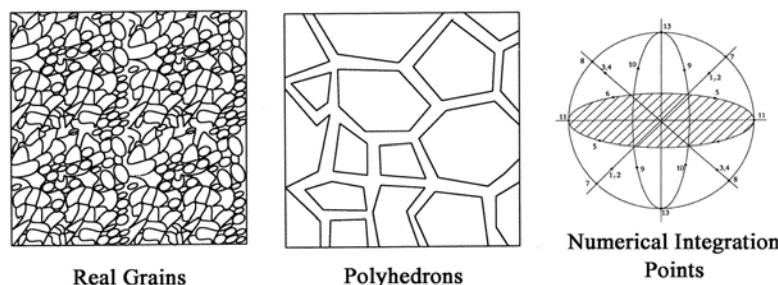


Fig. 2. Soil grains, artificial polyhedrons, and sampling points

In an ideal case, the normal integration is considered as summing up the individual micro effects corresponding to the infinite number of micro sampling planes.

The choice of 13 planes for the solution of any three dimensional problems is a fair number. The orientation of the sampling planes and direction cosines of two perpendicular on plane coordinate axes and weighted coefficients [23] for an employed numerical integration rule and the calculation of a stress tensor of each plane are shown in Fig. 3.

Upon yield criterion in plasticity, the stress condition exceeds the yield limits, plastic sliding or widening/closing take place as an active plane. Therefore, one of the most important features of a multi-plane framework is that it enables the identification of the active planes as a matter of routine. The application of any stress path is accompanied by the activities of some of the 13 defined planes at any point in the medium. The values of plastic strain on all the active planes are not necessarily the same. Some of these planes initiate plastic deformations earlier than others. These priorities and certain active planes can change due to any change of direction of the stress path. A number of active planes may stop activity, will some inactive ones become active, and some planes may take over others with respect to the value of the plastic shear strain. Thus the framework is able to predict the mechanism of failure.

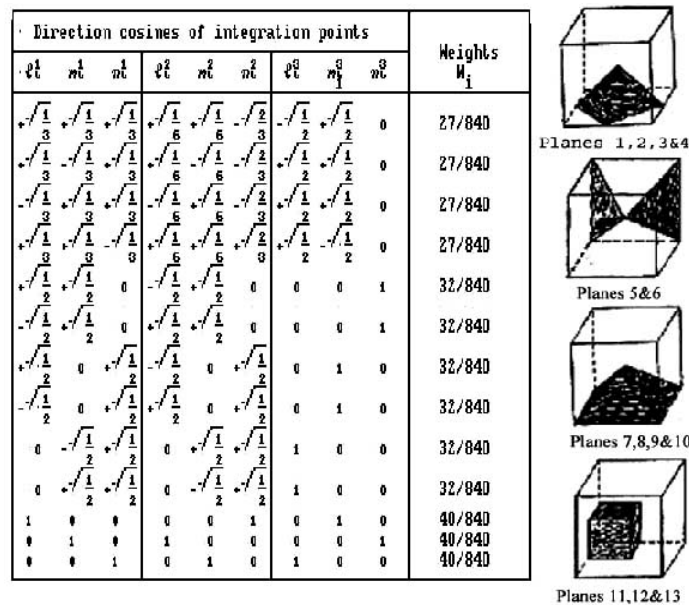


Fig. 3. Direction cosines, weighted coefficient, demonstration of 13 planes

4. STRENGTH ELLIPSOID

In general, a quantitative description of initial micro-fabric would enhance the characterization and forecasting of sand behaviour under different loading. On loading the fabric is continuously altered. Hence, it is necessary to develop techniques to quantify a changes in fabric as well. While the material is distorted, the fabric of the material changes and therefore, a strain or displacement field occurs in the material. Consequently, the strain and induced fabric of a material are inherently related to each other[24]. A popular approach for the formulation of strength criteria for anisotropy granular materials is the generalization of isotropic ones. Such a criterion is usually geometrically interpreted as a limiting envelope in a stress space, which means that a condition of failure occurs when a given stress vector touches the failure envelope. Since the condition for failure is intrinsic to the material, the failure criterion can be defined differently for any probable sliding plane through the material. Accordingly, the stress ratio can not exceed the corresponding value of $(\tan(\phi))$, neither on the planes of weakness nor on any other plane which does not tend to slide.

On a loading orientation inclined by three angles (direction cosines) with respect to the bedding plane, a certain sliding mechanism composed of active sliding planes provides a value of stress ratio which corresponds to the most active plane and has a limitation of $(\tan(\phi))$ that is governing sand strength against sliding. Therefore, on any orientation within the sand, the state of strength depends on the geometry of the bedding plane and the orientation of the applied load with respect to the bedding plane. To describe the strength, $(\tan(\phi))$, at any orientation, it is necessary to find a way of summarizing the configuration of different strengths corresponding to all probable directions passing through the medium.

For ideal granular media with no preferential orientation a spherical envelop of strengths $(\tan(\phi))$ may provide uniform sliding strength on any orientation. However, to consider fabric effects due to the bedding plane, an ellipsoidal envelop of strength may be the most suitable presentation of strength variation on different directions. The longest diameter of this ellipsoid is always normal to the bedding plane. Configuring the 13 predefined planes in the strength ellipsoid provides a certain elliptical section on each plane that presents the variation of strength with respect to the sliding orientation. In other words, the tips of the arrow heads of strength value of different orientations collectively define a built up geometrical surface called the strength ellipsoid. Obviously, the size of the strength ellipsoid of each plane is different and presents maximum and minimum strengths for sliding along the longest and shortest ellipse, respectively. The other sliding orientations are faced with strength limitations in between depending on the direction of shear stress on the plane with respect to the bedding plane.

Adopting the multi-plane mechanism of sliding planes configured in Fig. 3, with respect to the orientation of the applied major principal stress axis, these planes are configured in a symmetric manner around a major principal axis. Any change in the principal stress axis direction creates a new set of strength ellipses with different strengths against sliding directions on different planes.

Extensive similar aspects to this subject have been proposed by different authors [25, 26, 11-14]. Accordingly, the emphasis on these studies, were on the evolution from inherent to induced anisotropy. [8], proposed a diagram of frequency of contacts as a function of the orientation of their normals for direct shear test, both before and after shearing as fabric ellipsoid.

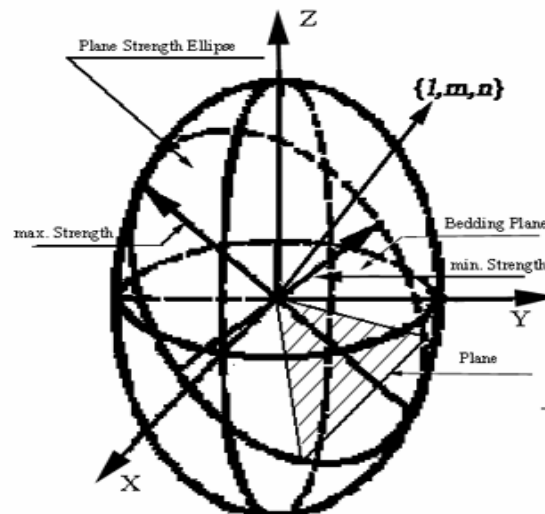


Fig. 4. Typical ellipse strength of a plane in ellipsoid strength
(Embedded plane assumed to be horizontal)

This study, carried out for the micro-fabric behaviour of loose, medium, and dense granular materials, led to the establishment of a statistical criterion of natural anisotropy based on the hypotheses that experience

accepted as probable. The fabric anisotropy law is represented as a spatial closed ellipsoid strength function in x , y , and z coordinates as follows:

$$x^2 / B + y^2 / B + z^2 / A - 1 = 0 \quad (1)$$

A , B , and C are three mutually perpendicular diameters of ellipsoid respectively. A construction of a typical ellipsoid is shown in Fig. 4.

Furthermore, to overcome the anisotropy concerning the loading orientation, a possibility of having all different probable sliding mechanisms must be provided in the used model. In this way, the application of any arbitrary loading or stress path leading to a certain sliding mechanism obeys the minimum energy level in natural law. These possibilities are provided in an elastic-plastic Multi-Plane model.

To find the strength ellipsoid diameters, two triaxial standard compression tests must be arranged; one with a horizontal bedding plane and vertical loading axis (test one), and the other with both a vertical bedding plane and a loading axis (test two). According to the author's experience (Sadrnejad (1997)) [26], in both of the two tests, planes 1 to 4 are mostly active, however in the second case, because of the 90 degree rotation of the load in axis, the smaller ellipse of strength on active planes is provided by the main strength ellipsoid. There, friction angles are applicable, while the loading axis is diverged with respect to the normal axis to the bedding plane. In a triaxial compression test, the sliding orientation on active planes is along the longest diameter of each plane strength ellipse. Furthermore, these four most activated planes in test one are symmetrically located around a loading axis that is identical with the normal line to the bedding plane. Therefore, for any axe-symmetry loading conditions similar to the triaxial compression test, there should be axe-symmetry of strength with respect to the normal axis to the bedding plane. In this case, the obtained φ value from the test and the coordinates of tip head arrows of shear strain on planes provide a unique equation which relates to the unknown strength ellipsoid parameters. However, due to axe-symmetry, two minor diameters of the strength ellipsoid are equal, so $B=C$. To find the coordinates of tip head arrows of shear strain, one simply can obtain the direction cosines of shear stress/strain on the corresponding plane, considering the length of the arrow to be equal to $\tan(\varphi)$, and one point of strength ellipsoid is known. It must be added that in triaxial standard tests, the coaxiality of strain and stress is valid, therefore, to obtain any active plane sliding it is enough to find the direction of corresponding shear stress. In the second compression test, the loading axis is rotated by 90 degrees, so the same active planes rotated by same angle and their strength ellipses as well. In this case, the geometry of strength ellipsoid is the same as test one. However, different $\tan(\varphi)$ and coordinates of tip head arrows are provided that lead to providing the second relation between strength ellipsoid parameters. The simultaneous solution of both equations presents the unknown parameters A , B , and C . Assuming the direction cosines of the advanced active planes in the first and second tests as ℓ, m, n and ℓ', m', n' , respectively, A and B are calculated as follows:

$$\begin{aligned} x_1^2 + y_1^2 + z_1^2 &= \tan^2(\varphi), \\ x_1'^2 + y_1'^2 + z_1'^2 &= \tan^2(\varphi') \end{aligned} \quad (2)$$

$$\begin{aligned} \frac{(\ell \tan\varphi)^2}{B^2} + \frac{(m \tan\varphi)^2}{B^2} + \frac{(n \tan\varphi)^2}{A^2} &= 1, \\ \frac{(\ell' \tan\varphi')^2}{B^2} + \frac{(m' \tan\varphi')^2}{B^2} + \frac{(n' \tan\varphi')^2}{A^2} &= 1 \end{aligned} \quad (3)$$

The simultaneous solution of two equation yields:

$$A = \frac{\sqrt{(\ell^2 + m^2)n^2 - n^2(\ell^2 + m^2)\tan(\varphi)\tan(\varphi')}}{\sqrt{(\ell^2 + m^2)\tan^2(\varphi) - (\ell^2 + m^2)\tan^2(\varphi')}} \quad (4)$$

$$B = \frac{\sqrt{(\ell^2 + m^2)n^2 - n^2(\ell^2 + m^2)\tan(\varphi)\tan(\varphi')}}{\sqrt{n^2 \tan^2(\varphi) - n^2 \tan^2(\varphi')}} \quad (5)$$

Performing a compression plane stress, the axe-symmetry condition is not available any more. The prevention of out of plane strain affects the activation and sliding orientation of planes. In this case, the conservation of the minimum level of energy law forces the mechanism to occur in a different manner as well as geometry. The change in the sliding orientation on an active plane from the first natural possible case may make a necessity of grain rolling under the constrained conditions. This may lead the sliding to face local interlocking, which generally appears as unstable higher friction angle φ_f , creating an unstable larger strength ellipsoid for these kinds of sliding planes. This unstable ellipsoid will disappear as soon as the stress path passing over the top peak shear strength, softening mode, and strength condition come back to a normal strength ellipsoid. Certainly, the larger strength ellipsoid provides a larger unstable intersection strength ellipse on the corresponding plane.

To find out the values of the internal friction of 13 planes oriented inside a certain strength ellipsoid, first the direction cosines of the stress vector as ℓ'_i, m'_i, n'_i are calculated as follows:

$$\beta_i = \arctan \left| \frac{\tau_x}{\tau_y} \right| \quad (6)$$

$$\begin{Bmatrix} \ell'_i \\ m'_i \\ n'_i \end{Bmatrix} = \begin{bmatrix} \cos \beta_i & 0 & -\sin \beta_i \\ 0 & 1 & 0 \\ \sin \beta_i & 0 & \cos \beta_i \end{bmatrix} \begin{Bmatrix} \ell_i \\ m_i \\ n_i \end{Bmatrix} \quad (7)$$

The value of $\tan(\varphi')$ in direction ℓ'_i, m'_i, n'_i is obtained as follows:

$$\tan(\varphi') = \frac{A.B}{\sqrt{(\ell_i'^2 + m_i'^2)A^2 + n_i'^2 B^2}} \quad (8)$$

The direction of the calculated shear stress on the i^{th} plane is associated with a certain value of internal friction angle φ_i in the strength ellipsoid. This friction angle can be obtained through the equation by intersection of the ellipse plane with the strength ellipsoid having the direction of shear stress direction cosines. Simply, any change of shear stresses on these planes results in new sliding mechanism and strengths.

5. CONSTITUTIVE EQUATIONS

Constitutive modeling of particulate material including different features has been the subject of numerous investigations during recent years, primarily because of the increasing awareness of the complexity of the loading conditions to which particulate material structures are subjected and the corresponding need for a more accurate analysis for the prediction of the safety of such structures. The parallel development of more powerful and efficient numerical methods of analysis has motivated and allowed the use of sophisticated constitutive models beyond the linear or simple non-linear elastic-plastic constitutive laws which were utilized in the early stages.

Most of the proposed models are based on the theory of elastic-plasticity, incorporating different yield criteria, flow and hardening rules. Strain hardening models according to various isotropic, kinematics or mixed hardening rules have been proposed. These models usually deal with a single or a combination of stress invariants. The principal axes rotation of stress/strain or both, and induced/inherent anisotropy have been observed in many tests. However, a model based on the invariant of the stress/strain tensors, therefore cannot cope with the real behaviour of particulate material such as soil under a complex loading program while either the values of stress or strain invariant are kept constant.

The first multi-laminate model was presented by Zienkiewicz *et al.* [27]. A multilaminate model for granular material was developed by Sadrnejad *et al.* and Sadrnejad. Also, a micro-plane model was developed by Bazant, *et al.*, [28].

For the soil mass, the overall stress-strain increments relation, to obtain elastic-plastic strain increments ($d\varepsilon^{ep}$), is expressed as:

$$d\varepsilon^{ep} = C^{ep} \cdot d\sigma \quad (9)$$

C^{ep} is the elastic-plastic compliance matrix. Clearly, it is expected that all effects and changes in elastic and plastic behaviour be included in C^{ep} . To find out C^{ep} , while decomposing the global behaviour into different sampling planes, the constitutive equations for a typical slip plane must be considered in the calculations. Consequently, the appropriate summation of all provided compliance matrices corresponding to the considered slip planes yields overall C^{ep} , therefore, the strain increment at each stress increment is calculated as follows:

$$d\varepsilon^{ep} = \frac{1}{8\pi} \sum_{i=1}^{13} W_i [L\varepsilon]^T C_i^{ep} [L\sigma] d\sigma' \quad (10)$$

$L\varepsilon$ and $L\sigma$ are transformation matrices for strain and stresses, respectively.

6. CONSTITUTIVE EQUATIONS FOR SAMPLING PLANE

A sampling plane is defined as a boundary surface that is a contacting surface between two structural units of polyhedral blocks. These structural units are parts of a heterogeneous continuum, for simplicity, defined as a full homogeneous and isotropic material. Therefore, all heterogeneities behaviour is supposed to appear in inelastic behaviour of the corresponding slip planes. In many cases, however, the medium is known to be heterogeneous and the notion of continuum is used to describe it on a scale much larger than the scale of the real particles. When this approach of 'pre-smoothing' is taken a priori, without any knowledge of the distribution and aggregation of specific microstructure, information on all internal detail, on the distribution of inter-granular stresses, strains and many other real features is forfeited. Since in reality this information is necessary to understand the overall deformation resistance of the soil, this aspect becomes too complicated. Therefore, the material that is contained inside a structural unit is treated as a 'black box'.

In many instances, the scale of the microstructure is coarse enough to be out of the range of such specific considerations of slip theory, and the individual component blocks can be considered as a continuum with well-defined plastic resistances and hardening behaviour. In this research, the individual component blocks of the overall media deform collectively as a heterogeneous (but compatible in deformations with other blocks) assembly of continua, interacting with each other only through the boundary conditions applicable at their various interfaces. The deformations of such coarse heterogeneous assemblies are best considered in full detail, preserving the information of the internal variations of effective deformational resistances in individual component blocks and associated internal stresses. This

can then be followed by an averaging or 'post-smoothing' approach, which permits the monitoring of the evaluation of internal deformations in addition to the overall deformation resistances [29].

The elastic-plastic constitutive equations of a sampling plane start with the classical decomposition of strain increments under the concept of elastic-plasticity in elastic and plastic parts are schematically written as follows:

$$d\varepsilon_i^{ep} = d\varepsilon_i^e + d\varepsilon_i^p \quad (11)$$

The increment of elastic strain ($d\varepsilon^e$) is related to the increments of effective stress ($d\sigma$) by:

$$d\varepsilon_i^e = [D_i^e]^{-1} d\sigma_i \quad (12)$$

$[D_i^e]^{-1}$ is a nonlinear elastic compliance matrix for the i^{th} plane and is usually obtained as follows:

$$[D_i^e] = (K_i - \frac{2}{3}G_i)\delta_{kk}\delta_{mn} + G(\delta_{kn}\delta_{im} + \delta_{km}\delta_{in}) \quad (13)$$

K_i and G_i are the bulk and the shear modulus for the i^{th} plane, respectively. Any kind of non-linearity as the change of these parameters may be applied in an incremental algorithm. A simple form of this change in shear and bulk modulus is as follows:

$$G_i / G_{i0} = P_a [(2.97 - e)^2 / (1 + e)] [\sigma_{ni} / P_a]^h \quad (14)$$

$$K_i = G_i \frac{2(1 + \nu)}{3(1 - \nu)} \quad (15)$$

G_{i0} and h are material properties, e is the void ratio and P_a is the atmospheric pressure. The bulk modulus may be computed by assuming a value for Poisson's ratio. The dilatancy factor for the i^{th} plane is defined as:

$$d_i = \frac{\delta\varepsilon_{in}^p}{\delta\varepsilon_{it}^p} = d_{i0} (e^{m\psi} - \eta_i / \eta_{ci}) \quad (16)$$

$\delta\varepsilon_{in}^p$ and $\delta\varepsilon_{it}^p$ are plastic normal and shear strain components on the i^{th} plane, respectively. d_{i0} and m are two material constant obtained in calibration. η_i and η_{ci} are stress ratio (τ_i / σ_{ni}) and the slope of the steady state line that is a certain percentage of $\tan(\varphi_{fi})$ for the i^{th} plane. ψ is the steady state parameter and is assumed to be equal for all planes and is calculated as follows:

$$\Psi = e - e_{cr} \quad (17)$$

e_{cr} is the critical void ratio that is obtained as follows:

$$e_{cr} = e_{\Gamma} - \lambda_C (p' / q)^{\xi} \quad (18)$$

e_{Γ} , ξ and λ_C are macroscopic material constants.

The yield criterion is locally defined by the ratio of the shear stress component (τ_i) to the normal effective stress (σ'_{ni}) on the i^{th} sampling plane. The simplest form of yield function, i.e. a straight line on τ versus σ_n space, is adopted. As the ratio τ/σ_n increases, the yield line rotates anti-clock-wise due to hardening and approaches Mohr-Coulomb's failure line and finally failure on corresponding plane takes place. The equation of yield function is formulated as follows:

$$f_i(\tau_i, \sigma_{ni}, \eta_i) = \tau_i - C'_i - \eta_i \sigma_{ni} \quad (19)$$

C'_i is cohesion of soil for the i^{th} plane.

A loading parameter, L_i is defined for the i^{th} plane as follows [30]:

$$L_i = 1/K_{pi}((\partial f_i/\partial \sigma'_{ni})d\sigma'_{ni} + (\partial f_i/\partial \tau_i)d\tau_i) = (d\tau_i - \eta_i d\sigma'_{ni})/K_{pi} = (\sigma'_{ni} d\eta_i / K_{pi}) \quad (20)$$

is calculated as follows:

$$K_{pi} = [h_1 - h_2 e] G_i ((\eta_{ci} / \eta_i) - e^{n^v}) \quad (21)$$

n , h_1 and h_2 are material constants. The elastic-plastic strain components for the i^{th} plane are calculated as follows:

$$d\varepsilon_{it}^{ep} = d\varepsilon_{it}^e + d\varepsilon_{it}^p = \frac{d\tau_i}{3G_i} + \frac{d\sigma'_{ni}\eta_i}{K_{pi}} = \left(\frac{1}{3G_i} + \frac{1}{K_{pi}} \right) d\tau_i - \frac{\eta_i}{K_{pi}} d\sigma'_{ni} \quad (22)$$

$$d\varepsilon_{in}^{ep} = d\varepsilon_{in}^e + d\varepsilon_{in}^p = \frac{d\sigma'_{ni}}{K_i} + d_i d\varepsilon_{it}^p = \frac{d_i}{K_{pi}} d\tau_i + \left(\frac{1}{K_i} - \frac{d_i \eta_i}{K_{pi}} \right) d\sigma'_{ni} \quad (23)$$

These equations are written in matrix form as:

$$\begin{Bmatrix} d\varepsilon_{it}^{ep} \\ d\varepsilon_{in}^{ep} \end{Bmatrix} = \begin{bmatrix} \frac{1}{3G_i} + \frac{1}{K_{pi}} & -\frac{\eta_i}{K_{pi}} \\ \frac{d_i}{K_{pi}} & \frac{1}{K_i} - \frac{d_i \eta_i}{K_{pi}} \end{bmatrix} \begin{pmatrix} d\tau_i \\ d\sigma'_{ni} \end{pmatrix} \quad (24)$$

Consequently, the elastic-plastic compliance matrix for the i^{th} plane is written as follows:

$$C_i^{ep} = \begin{bmatrix} \frac{1}{3G_i} + \frac{1}{K_{pi}} & -\frac{\eta_i}{K_{pi}} \\ \frac{d_i}{K_{pi}} & \frac{1}{K_i} - \frac{d_i \eta_i}{K_{pi}} \end{bmatrix} \quad (25)$$

This 2×2 matrix can be transformed into a 6×6 matrix in global coordinates as the effect of the i^{th} plane in the mechanical behaviour of a typical point. Any kind of instabilities, softening, ill-conditioning, limitation in tensile/shear strength of the i^{th} plane can be included in this matrix.

$$C_{-i}^{ep} = [T_i] C_i^{ep} [T_i]^{-1} \quad (26)$$

Therefore, the global compliance matrix based on multi-plane numerical integration is found as follows:

$$C^{ep} = 8\pi \sum_{i=1}^{13} W_i C_{-i}^{ep} \quad (27)$$

7. VERIFICATION OF MODEL RESULTS

The test result on Toyoura sand, whose specific gravity is 2.66 g/cm^3 , was employed for the verification of the proposed model. The maximum void ratio e_{max} of this sand was 0.977 and e_{min} was 0.597. The grain size distribution curve is shown in Fig. 6.

The mean grain size D_{50} was 0.20 mm, and the uniformity coefficient was 1.24. Linear variations of e_{ph} and e_f versus $(P/P_a)^\xi$, as presented by Li *et al.*, are adopted [31].

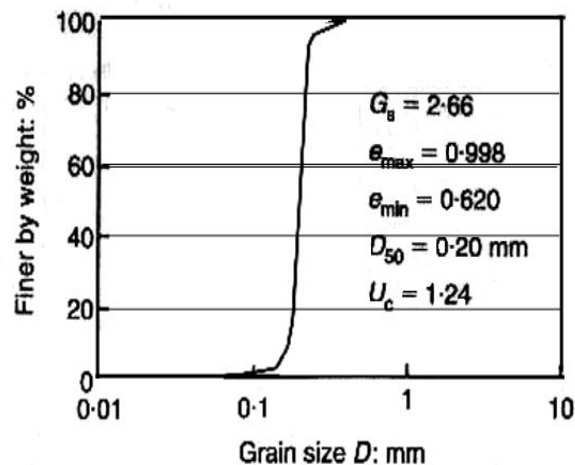


Fig. 5. The grain size of Toyoura sand

8. IDENTIFICATION OF PARAMETERS

For an axis-symmetry anisotropy of soil that is more practical, two triaxial standard compression tests upon the horizontal and vertical bedding plane is enough to identify A , B , and C . The strength and dilation parameters of the multi-plane model are G_0 , ν , ϕ_{fi} , η_{ci} , e_r , λ_C , ξ , d_0 , h_1 , h_2 and n . The first two parameters correspond to the elastic behaviour of the soil skeleton. ϕ_{fi} is obtained from the built up strength ellipsoid on the corresponding bedding plane for 13 planes as presented in [7].

The ratio of $\eta_{ci}/\tan(\phi_i)$ is assumed initially the same for all directions. This ratio is obtained during the calibration of stress-strain of triaxial standard tests. This parameter is assumed to vary after exceeding the phase transformation line to exceed one. This variation means that the strength ellipsoid approaches the sphere at failure condition. Certainly, there should be a continuous reform of this ellipsoid due to the rotation of principal effective stress axes, however, to ease the solution, this variation can be neglected up to the steady state line. Accordingly, this reform has been considered during post-liquefaction.

Starting from the hydrostatic initial stress condition and no plastic strain history, these parameters, except for friction angles, are assumed to be the same for all planes and are found by numerical calibration with the results of the stated two triaxial compression tests.

The parameters found for Toyoura sand by calibration are: $G_0=245$ MPa., $\nu=0.3$, $\eta_{ci}=0.6$, $e_r=0.934$, $\lambda_C=0.019$, $\xi=0.7$, $d_0=4.6$, $m=5.4$, $h_1=3.15$, $h_2=3.55$ and $n=1.1$. $(\tan(\phi_i))_{\max}=0.8665$, and $(\tan(\phi_i))_{\min}=0.7602$. $A=0.8563$, $B=C=0.7752$, [7].

To present the ability of the proposed model, the test results conducted by Verdugo & Ishihara [32] on Toyoura sand are produced by the model. The obtained model results through the use of calculated parameters are presented as the comparison of stress deviator versus effective mean stress (stress paths), and stress deviator versus axial strain.

Figure 7a, b, shows the comparison stress paths of the model result with tests for dense Toyoura sand as stress deviator versus different initial mean stress. Also, the comparison of stress deviator versus axial strains are shown in Fig. 8a, b. The comparison of the stress path for loose Toyoura sand are shown in Fig. 9a, b. The comparison of stress deviator versus axial strain for loose sand is shown in Fig. 10a, b.

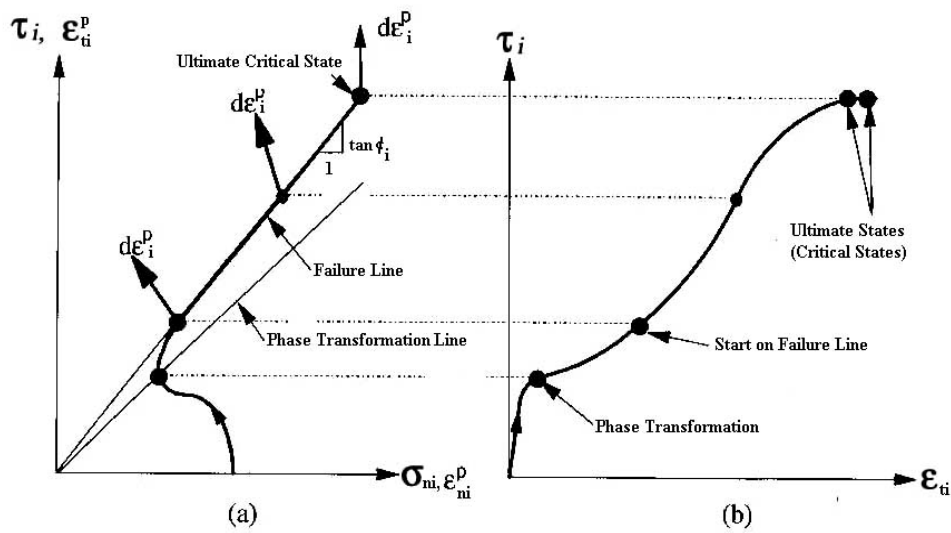


Fig. 6. Undrained stress path and stress-strain on a plane

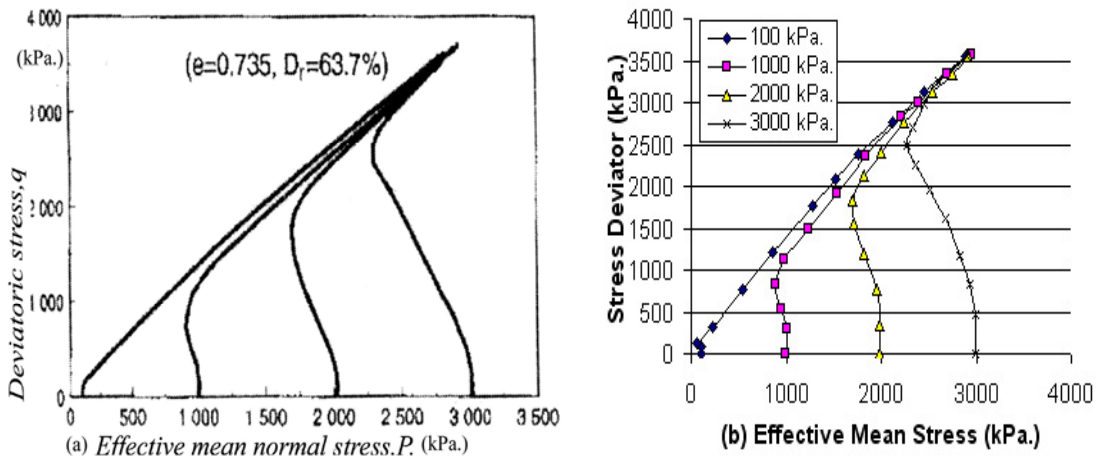


Fig. 7. Comparison of experimental with model results ($e=0.735, D_r=63.7\%$),
a) test results, b) model results

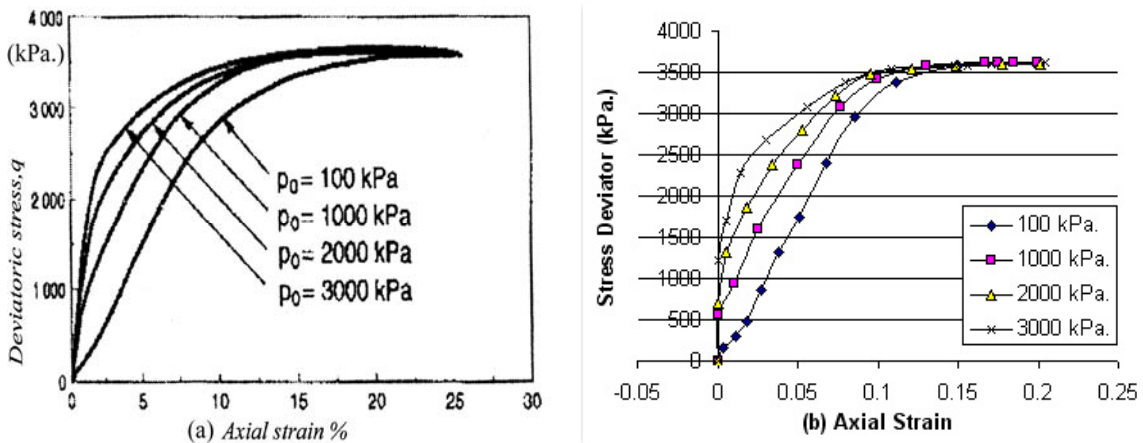


Fig. 8. Comparison of experimental with model results (different initial mean stress),
a) test results, b) model results

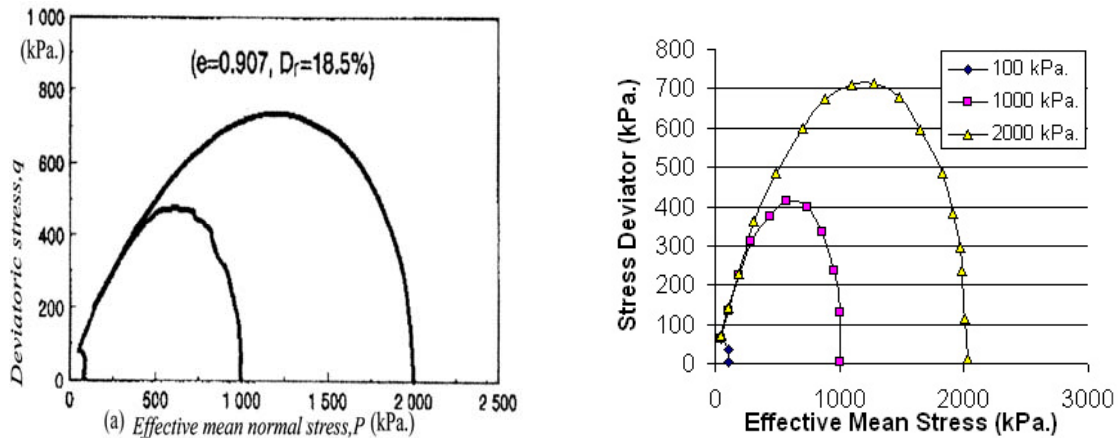


Fig. 9. Comparison of experimental with model results ($e=0.907, D_r=18.5\%$), a) test results, b) model results

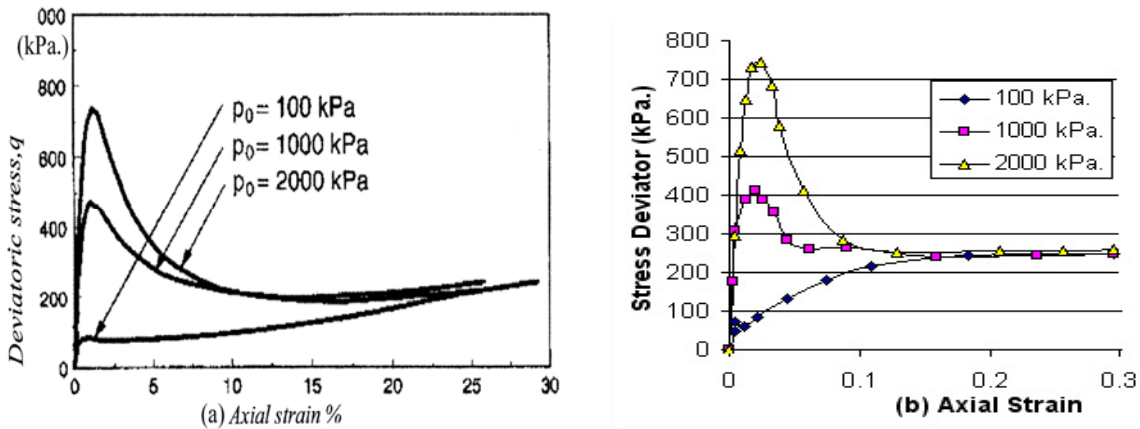


Fig. 10. Comparison of experimental with model results ($e=0.907, D_r=18.5\%$, and different initial mean stress), a) test results, b) model results

To show the capability of the proposed model in predicting the effects of bedding plane and changes in the orientation of principal stress axes, the hollow cylindrical test results presented by Nakata, *et al.* [33] were produced and compared with the test results. Figure 11-a to 11-f show like to like comparisons

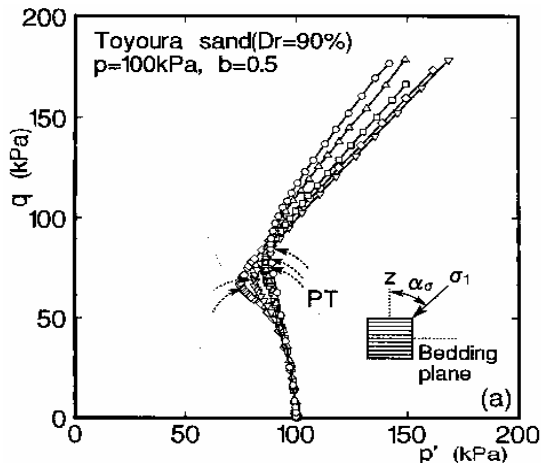


Fig. 11. a1 (Nakata, *et al.* [34])

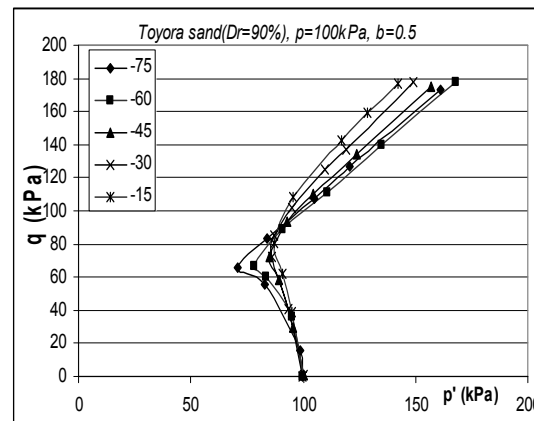


Fig. 11. a2 (Model results)

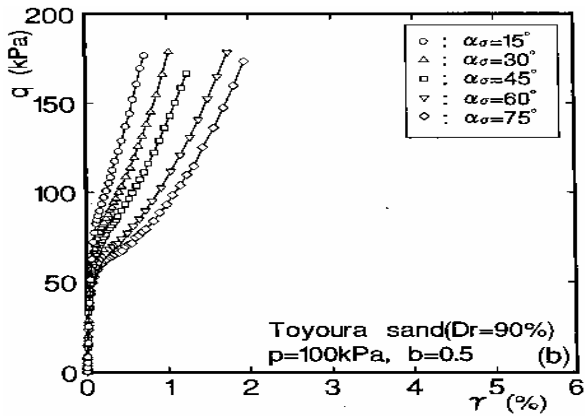


Fig. 11. b1(Nakata, *et al.* [34])

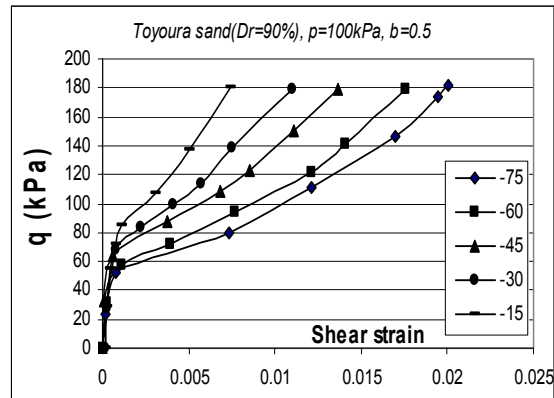


Fig. 11. b2 (Model results)

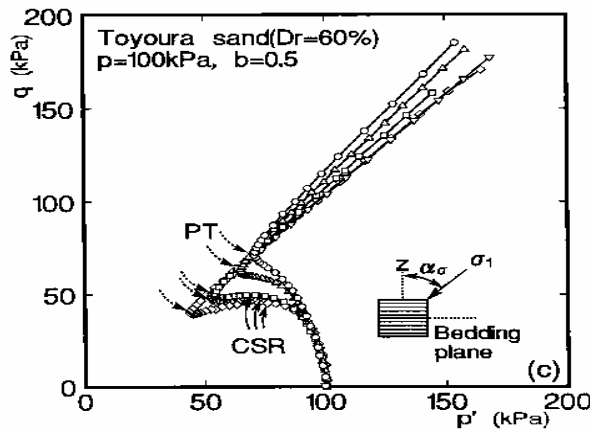


Fig. 11. c1(Nakata, *et al.* [33])

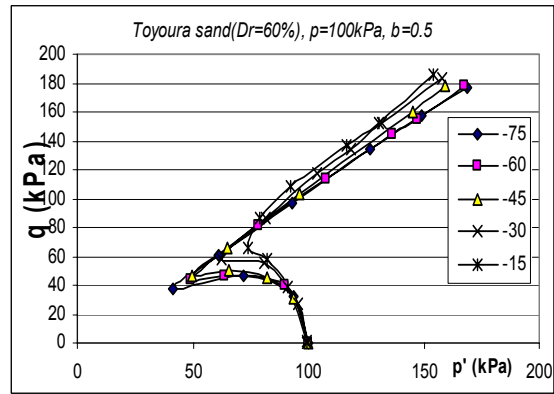


Fig. 11. c2 (Model results)

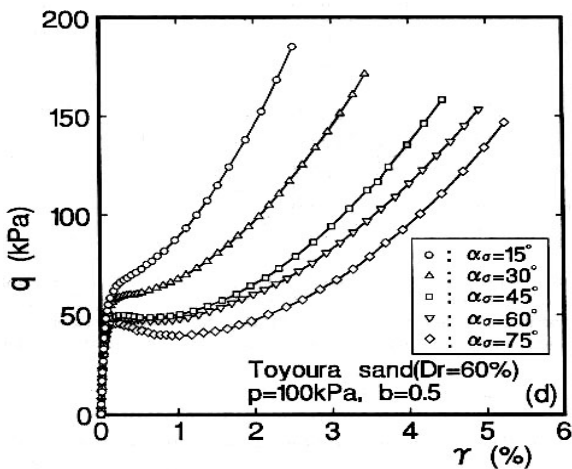


Fig. 11. d1(Nakata, *et al.* [34])

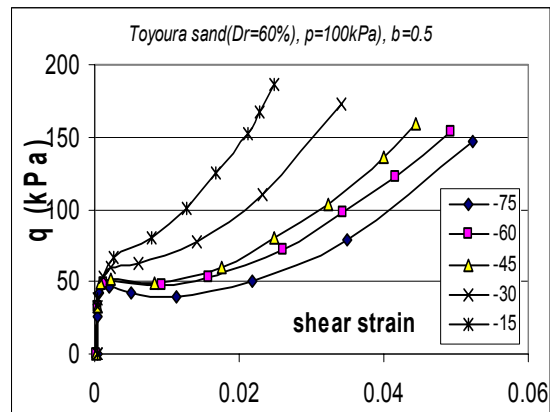


Fig. 11. d2 (Model results)

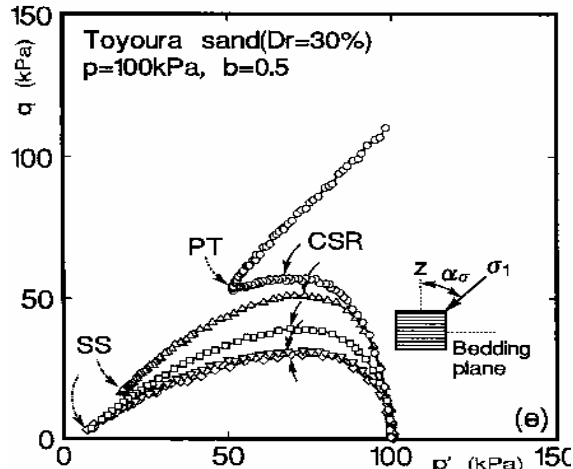


Fig. 11. e1(Nakata, *et al.* [34])

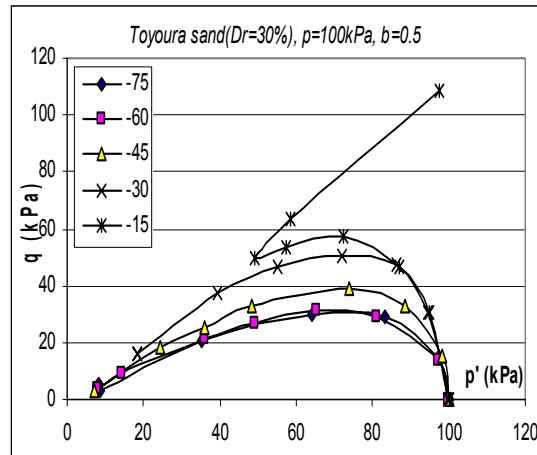


Fig. 11. e2 (Model results)

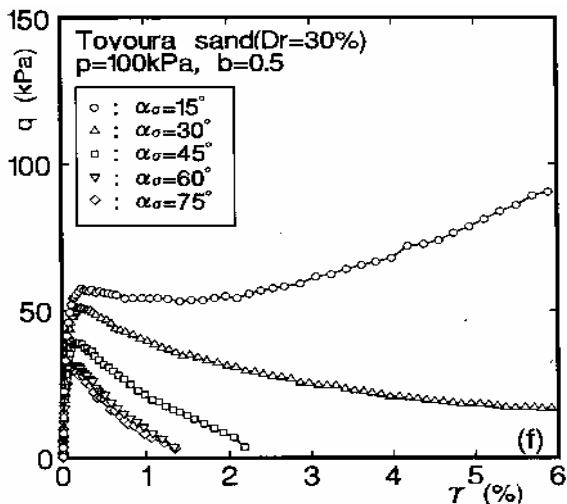


Fig. 11. f1 (Nakata, *et al.* [34])

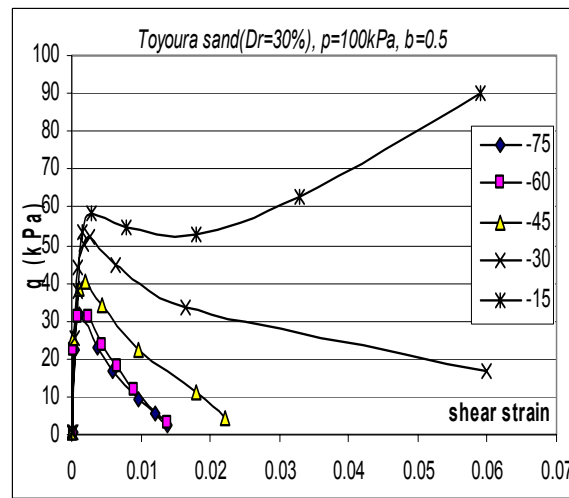


Fig. 11. f2 (Model results)

These comparisons show that the model has predicted tally results as the effects of principal stress axes orientation on the mechanical behaviour of Toyoura sand.

An important feature is that the developed model sets plasticity formulation for smooth transitions between the elastic and plastic states, making it advantageous in cyclic simulations. Hysteresis loops and plastic strain increments for successive cycles can be described in a relatively simple manner. The concept allows formulation which may be important to simulate variations in soil skeleton behavior during cyclic loading. An undrained cyclic triaxial compression test reported by Towhata and Ishihara [34] was predicted and well compared with the test in Fig. 12. The stress path of six cycles of loading/unloading/reloading and the corresponding variation of shear stress vs. shear strain led to the zero effective mean stress obtained by the proposed model and are plotted and located in front of the above experimental results. This general comparison shows that the model results are similar to the experiment with a minor and very little diversion. Consequently, the proposed model can be used to predict the cyclic behavior of sand.

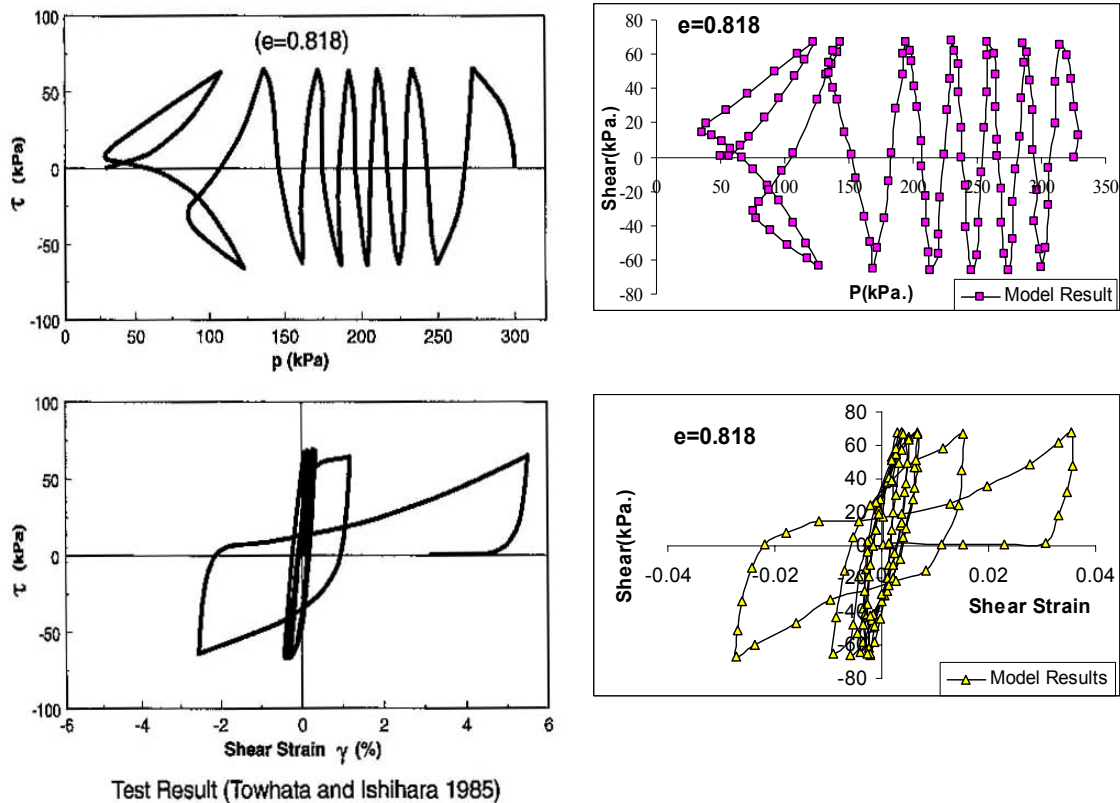


Fig. 12. The comparison of Undrained cyclic triaxial compression test reported by Towhata and Ishihara [34] with model results

9. CONCLUSION

A multi-plane based model incorporating the steady/critical state concept was developed for the undrained behaviour of sand for post liquefaction. The main feature of this model is the use of a pressure dependent peak stress ratio parameter that approaches the steady/critical state value as the steady/critical state normal stress is approached. The model was shown to be capable of accurately predicting the undrained behaviour of sand over a wide stress region.

A method to solve anisotropy of soil as the effects of natural micro-fabric and also due to inclination of direction of the applied load with respect to the bedding plane is presented and verified. This method is simple, and based on the minimum energy level in natural law. Despite the directional effect on soil strength, the presented distribution of strength by the rotation of the bedding plane is of a unique form through the material. This aspect simplifies the use of the presented method to find strength ellipsoid parameters.

A micro-plane numerical algorithm is also presented for a better anticipation of load inclination effects through the material. In this way, the directional information and effects of applied load orientation on mechanical behaviour of material are addressed and considered. Further than the possibility of predicting inherent anisotropy, this rational way facilitates the model to predict the effects of stress/strain principal axes rotation, induced anisotropy and a potential to solve the anisotropy of the material through defining different mechanical behaviour on different orientation. This is achieved by the use of a generally simplified, applicable, effective, and easily understandable relation between micro and macro scales. These relations demonstrate an easy way to handle any heterogeneous material property as well as mechanical behaviour of materials.

This model is able to solve a three dimensions plasticity problem by a rather simple theory based on the phenomenological description of two dimensions plastic deformation and kinematics hardening of materials. This is actually achieved in such a way that the application of some difficult tasks such as induced and inherent anisotropy and the rotation of principal stress and strain axes where there may not be co-axiality among them during plastic flow, can be predictable. Accordingly, the sampling plane constitutive formulations provide a convenient means to classify loading events, generate history rules, and formulate independent evolution rules for local variables.

REFERENCES

1. Li, X. S. & Dafalias, Y. F. (2000). Dilatancy for cohesionless soils. *Geotechnique. J.*, 50(4).
2. Manzari, M. T. & Dafalias, Y. F. (1997). A critical state two surface plasticity model for sands. *Geotechnique*, 47(2), 255-272.
3. Wan, R. G. & Guo, P. J. (1997). Coupled dilatancy-compaction model for homogeneous and localized deformation of granular materials. *Numerical Methods in Geomechanics*, Pietruszczak & Pande, eds, Balkema, Rotterdam, 3-8.
4. Li, X. S. & Dafalias, Y. F. (2000). State- dependent dilatancy in critical-state constitutive modeling of sand. *Can. Geotech. J.*, 36(4).
5. Pooroshab, H. B. (1989). Description of flow of sand using state parameters. *Computers and Geotechniques*, 8, 195-218.
6. Been, K. & Jefferies, M. G. (1985). A state parameter for sands. *Geotechnique .J.*, 35(2).
7. Sadrnejad, S. A. (2001). A semi-micro-mechanical model for anisotropy of sand. *First Conference on Optimum Use of Land*, Teheran, Iran, 437
8. Oda, M. (1978). Significance of fabric in granular material. *Proc., US-Japan Sem. Mech. Gran. Mat.* 7-26.
9. Arthur, J. R. F. & Menzeis, B. K. (1972). Inherent anisotropy in a sand. *Geo-technique*, 22(1), 115-128.
10. Oda, M. & Koishikawa, I. (1977). Anisotropic fabric of sand. 9th *ICSMFE*, 1, 235-238.
11. Oda, M. (1972). Initial fabrics and their relations to mechanical properties of granular material. *Soils and Foundations*, 12(1), 17-36.
12. Oda, M. (1972). The mechanism of fabric changes during compressional deformation of sand. *Soils and Foundations*, 12(2), 1-18.
13. Oda, M. (1972). Deformation mechanism of sand in triaxial compression tests. *Soils and Foundations*, 12(4), 45-64.
14. Oda, M., Konishi, J. & Nemat Nasser, S. (1980). Some experimentally based fundamental results on the mechanical behaviour of granular materials. *Geotechnique*, 30, 479-495.
15. Oda, M. (1982). Geometry of discontinuous and its relation to mechanical properties of discontinuous materials. *IUTAM, Conference Deformation Failure of granular Materials*, Delft, Vermeer, Luger (eds), A.A. Balkema, Rotterdam, 93-99.
16. Sadrnejad S. A. & Pande G. N. (1989). A multi-laminate model for sand. *Proceeding of 3rd International symposium on Numerical Models in Geo-mechanics*, NUMOG-III, Niagara Falls, CANADA.
17. Sadrnejad, S. A. (1992). Induced anisotropy prediction through plasticity. *Proceeding of International Conference on Engineering Applications of Mechanics*, Teheran-Iran, 598-605.
18. Sadrnejad, S. A. (1992). Multi-laminate elasto-plastic model for granular media. *Journal of Engineering, Islamic Republic of Iran*, 5(1&2).
19. Sadrnejad S. A. (1998). Prediction of the rotation of principal stress axes in porous media by multi-laminate based model, *Int. Journal of Univ. of Science & Tech. of Iran*, 9(1), 15-33.

20. Sadmezhad, S. A. (1999). A multi-laminate elastic-plastic model for liquefaction of saturated sand. *Proceeding of the Third International Conference on Seismology and Earthquake Engineering*, I. R. Iran, 561-568.
21. Christofferson, C., Mehrabadi, M. M. & Nemat-Nasser, S. A. (1981). Micromechanical description of granular behaviour. *J. Appl. Mech.*, 48, 339-344.
22. Nemat-Nasser, S. & Mehrabadi, M. M. (1983). Stress and fabric in granular masses, *Mechanics of granular Materials. New Models and Constitutive Relations* (Eds. J.T. Jenkins and M. Satake), 1-8, Elsevier Sci. Pub.
23. Brewer, R. (1964). *Fabric and mineral analysis of soils*. Wiley, 129-158.
24. Abramowitz, M. & Stegun, I. A. (1965). *Handbook of mathematical functions*. Dover Publications, inc., Newyork.
25. Gerrard, C. M. (1977). *Background to mathematical modeling in geo-mechanics*. The role of fabric and stress history, in finite element in geo-mechanics, ed. G. Gudus, John. Wiley, 33-120.
26. Sadmezhad S.A. (1997). Numerical Identification of Failure Specifications of Soil. *4thInternational Conference on Civil Engineering*, 4-6 May 1997, Teheran, Iran, p. 100-111.
27. Zienkiewicz, O. C. & Pande, G. N. (1977). Time dependent multi-laminate model of rocks. *International Journal of Numerical and Analytical Methods In Geo-mechanics*, 1, 219-247.
28. Bazant Z. P. & Oh, B. H. (1983). Micro-plane model for fracture analysis of concrete structures. *Proceeding Symposium on the Interaction of Non-nuclear Munitions with Structures, held at US Air Force Academy*, Colorado Springs, May 1983, Published by: McGregor & Werner, Washington DC.
29. Sadmezhad, S. A. (2001). A semi-micro-mechanical model for anisotropy of sand. *First Conference On Optimum Use Of Land*, Teheran, Iran, 437.
30. Dafalias, Y. F. (1986). An anisotropic critical state soil plasticity model. *Mech. Res. Commun. J*, 6.
31. Li, X. S. & Dafalias, Y. F. (1999). State- dependent dilatancy in critical- state constitutive modeling of sand. *Can. Geotech. J.*, 36(4).
32. Verdugo, R. & Ishihara, K. (1996). The setady state of sandy soils. *Soils and Foundations*, J. 36(2).
33. Nakata, Y., Hyodo, M., Murata, H. & Yasufuku, N. (1998). Flow deformation of sands subjected to principal stress rotation. *Soils and Foundations*, 38(2), 115-128.
34. Towhata, I. & Ishihara, K. (1985). *Fifth International Conference on Numerical Methods in Geomechanics*, Nagoya, 523-530.